



Electron momentum spectroscopy study on valence electronic structures of pyrimidine

C.G. Ning*, K. Liu, Z.H. Luo, S.F. Zhang, J.K. Deng*

Department of Physics, Key Laboratory of Atomic and Molecular NanoSciences of MOE, Tsinghua University, Beijing 100084, People's Republic of China

ARTICLE INFO

Article history:

Received 31 March 2009

In final form 9 June 2009

Available online 12 June 2009

ABSTRACT

The momentum distributions of valence orbitals of pyrimidine were measured at various impact energies. The observed distributions were compared with HF, DFT-B3LYP, and OVGf calculations. The HOMO was unambiguously assigned to the $7b_2$ symmetry. It was found that the pole strength of the outer valence orbital $2b_1$ was 0.8. Moreover, the present study indicated that we should be very cautious in using the (e, 2e) reaction to investigate the molecular conformational population by comparing the PWIA theoretical results with the experimental results at a single impact energy.

© 2009 Elsevier B.V. All rights reserved.

1. Introduction

The properties and functions of molecules largely depend on their electronic structures. A detailed understanding of electronic structures of molecules with biological importance is of considerable interest and also fundamentally important [1,2]. Recently, Holland et al. reported the electronic structures of a variety of basic bio-chemical molecules using synchrotron radiation photoelectron spectroscopy [3]. The electron momentum spectroscopy (EMS) is an experimental technique capable of measuring the electron binding energies and momentum density distributions of the individual atomic or molecular orbitals [4,5]. The great potential of EMS on studying biological molecules was firstly demonstrated by Brion et al. in their seminal work of glycine, the simplest amino acid [6]. Here we reported the EMS investigation of valence electronic structures of pyrimidine. Pyrimidine is of great importance in biochemistry because it forms fundamental structures of bases in the nucleic acids DNA and RNA, such as thymine and uracil.

The valence binding energies of pyrimidine have been previously investigated using photoelectron spectroscopy with the HeI radiation [7–9]. Recently, Potts et al. extensively studied the valence electronic structures of pyrimidine using the synchrotron radiation incorporating Hartree–Fock (HF), OVGf and the third-order algebraic diagrammatic construction (ADC(3)) theoretical interpretations [10]. More recently, Lottermoser et al. investigated the valence ionization energies of pyrimidine and its various substituted derivatives in comparison with the density functional theory [DFT] [11].

In this Letter, we reported the first EMS study of the complete valence region of pyrimidine at the electron impact energies of

600 eV and 1500 eV. We compared the measured results against the Hartree–Fock and DFT calculations with more complete basis sets. The comparison between experimental momentum distributions and calculations of individual orbitals can provide very direct orbital assignment [12–14]. The observed dependence on impact energies of momentum distributions for some orbitals reflected the limitation of the plane wave impulse approximation (PWIA) for these orbitals.

2. Experimental and theoretical methods

The details of our high resolution electron momentum spectrometer have been reported elsewhere [15,16], so only a brief description was given here. Our spectrometer takes the symmetric non-coplanar geometry, also named the Weigold configuration [4]. The two outgoing electrons have almost equal energies and essentially equal polar angles ($\theta_1 \approx \theta_2 = 45^\circ$) respect to the direction of the incident electron beam. The double toroidal energy analyzer equipped with two large position sensitive detectors greatly increases the collecting efficiency for the coincidental (e, 2e) events. The momenta of electrons prior to being collided out can be determined through the out-of-plane azimuthal angle ϕ between the two outgoing electrons using the equation:

$$p = \sqrt{(p_0 - \sqrt{2}p_1)^2 + 2p_1^2 \sin^2 \frac{\phi}{2}}, \quad (1)$$

where p_0 and p_1 are the momenta of the incident electron and the outgoing electron, respectively.

In present experiment, the electron gun equipped with an oxide cathode was employed, which can generate an electron beam with a low energy spread and a low divergence angle due to the low working temperature (~ 1100 K). The space charge effects may largely broaden the energy distribution profile of the electron beam, thus deteriorate the energy resolution. In present work, a typical

* Corresponding authors. Fax: +86 10 62781604.

E-mail addresses: ningcg@tsinghua.edu.cn (C.G. Ning), djk-dmp@tsinghua.edu.cn (J.K. Deng).

electron beam into the Faraday cup is kept around 1.0 μA at the impact energy of 1500 eV plus binding energies, and around 0.3 μA at 600 eV. The energy resolution of 0.68 eV (full width at half maximum, FWHM) was obtained through the calibration run on Ar sample. The experimental momentum distributions at different impact energies were compared in order to check the validity of the plane wave impulse approximation (PWIA). It was recently found that the PWIA failed for some molecular orbitals, such as the highest occupied molecular orbital of oxygen [17], and the $1b_{3g}$ orbital of ethylene [18].

The commercial pyrimidine sample with a claimed purity of 99% was used without further purification. The absorbed gas was removed through several cycles of freezing–pump – thaw process. The needle valve, which controlled the flow rate of pyrimidine from the reservoir to the interaction region, was heated to 10 °C above the room temperature in order to prevent the fluctuation of the flow rate due to the possible condensation of pyrimidine.

Interpretation of the experimental results of EMS is usually taken under the plane wave impulse approximation (PWIA). Within the PWIA framework, and the target Hartree–Fock approximation (THFA) or the target Kohn–Sham approximation (TKSA), the differential EMS cross sections for randomly oriented molecules at gas phase are given by [19,20]

$$\sigma_{\text{EMS}} \propto S_i^f \int d\Omega |\psi_i(p)|^2, \quad (2)$$

where $\psi_i(p)$ is the momentum space representation of a canonical Hartree–Fock or Kohn–Sham orbital, and S_i^f denotes the associated spectroscopic factor, which accounts for the shake-up and shake-off processes due to configuration interactions in the final state.

The *ab initio* calculations discussed in the present work have been performed using GAUSSIAN program [21]. The theoretical momentum distributions were generated using our newly developed program named NEMS [22], which makes use of a general analytic formula for handling basis functions regardless of the angular momentum characterizing the atomic orbital functions, and which enables therefore treatments of basis sets incorporating formally any type (*s, p, d, f, g, h, i, ...*) of atomic functions.

3. Results and discussion

The binding momentum–energy density map of pyrimidine in the region of 5–35 eV at the electron impact energy of 600 eV was presented in the top of Fig. 1. The qualitative characteristics of each orbital can immediately be obtained from this map. For example, the orbitals with binding energies less than 12 eV are *p*-type, i.e. they have a minimum intensity at the azimuthal angle $\phi = 0^\circ$, which reflects that these orbitals are anti-symmetric in position space. The binding energy spectrum shown in the bottom was obtained by summing over all ϕ angles from the momentum–energy density map. The assignment for each peak was also labeled on the spectrum. It should be noted that our notation is different from that on the photoelectron spectra given by Potts et al. because they used a lower C_s symmetry in order to interpret their observed asymmetry parameter β , although pyrimidine molecule belongs to the C_{2v} point group. Six peaks can be resolved from the spectrum in the outer valence region (<18 eV). It can be seen that, in contrast to the sharp peaks in the outer valence region, only some weak peaks can be discerned on a continuum of background in the inner valence region (>20 eV). It is due to the severe breakdown of the single orbital image in the inner valence region. These observed binding energies for each peak were listed in Table 1 along with the PES and theoretical results. It should be noted that the HF method with the augmented Dunning's correlation consistent basis set Aug-cc-pVTZ [21] gives a different orbital order from

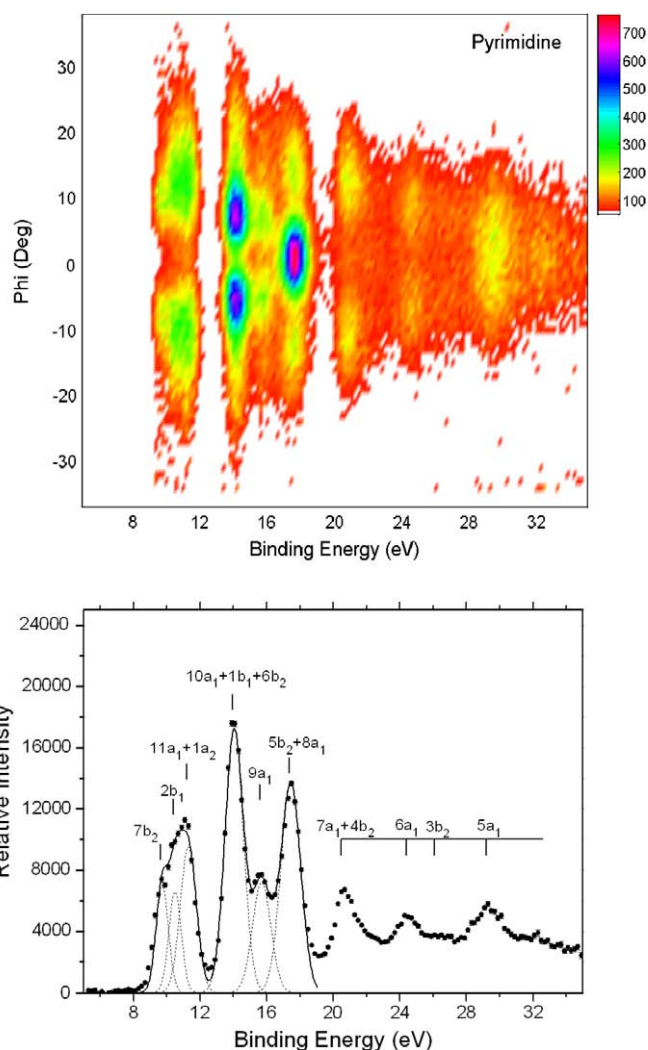


Fig. 1. Binding energy spectra of pyrimidine. The valence momentum–energy density map of pyrimidine measured at the impact energy of 600 eV plus binding energies (top); experimental binding energy spectra summed over all azimuthal angles (bottom).

Table 1
Ionization potentials of pyrimidine (in eV).

Orbital	PES ^a	EMS ^b	HF	B3LYP ^c	SAOP ^c	OVGF	ADC(3) ^a
7b ₂	9.8	9.8	11.34	7.29	10.29	9.83	9.49 (12a')
2b ₁	10.5	10.5	10.32	8.19	11.50	10.40	10.37 (3a'')
11a ₁	11.2	11.3	12.92	8.60	11.53	11.36	10.93 (11a')
1a ₂	11.5		11.56	9.04	12.30	11.28	11.20 (2a'')
10a ₁	13.9	14.1	16.00	11.55	14.27	14.49	14.40 (1a'')
1b ₁			15.77	11.76	14.91	14.49	14.42 (10a')
6b ₂	14.4		16.25	12.00	14.49	14.63	14.63 (9a')
9a ₁	15.8	15.7	17.76	13.09	15.79	16.25	16.26 (8a')
5b ₂	17.0	17.5	19.18	14.39	16.92	17.26	17.55 (7a')
8a ₁	17.7		20.16	15.00	17.56	18.25	18.11 (6a')
7a ₁		20.6	24.31	18.24	20.60		
4b ₂			24.41	18.27	20.65		
6a ₁		24.5	29.32	21.95	24.13		
3b ₂		26.2	32.62	24.61	26.61		
5a ₁		29.3	35.82	27.25	29.11		

^a See Ref. [10]. The notation with a lower C_s symmetry was used by Potts et al. in order to interpret their observed asymmetry parameter β . See texts for details.

^b Present work.

^c The difference between the DFT-B3LYP orbital energies and experimental ionization potentials was mainly due to the asymptotic error, which can be corrected by the statistical average of orbital potential method (SAOP) [31]. See texts for details.

that of the density functional theory with the standard hybrid Becke, three-parameter, Lee–Yang–Parr (B3LYP) exchange–correlation functional [23] and the outer valence green's function (OVGF) [24,25] with the Pople 6–311++G** basis set [21]. As an example, HF assigns the highest occupied molecular orbital (HOMO) to the $2b_1$ symmetry, while B3LYP assigns it to the $7b_2$ symmetry. The outermost peak at 9.8 eV related to HOMO can be confidently assigned to $7b_2$ symmetry through the comparison of the experimental momentum profiles with the theoretical ones, as shown in Fig. 2. The theoretical momentum distributions have taken the experimental momentum resolution at the impact energy of 1500 eV into consideration using the Monte Carlo method [26]. Since the experimental intensity is on a relative scale, the experimental momentum profile needs a normalization procedure in order to be compared with the theoretical one. In present work, as Fig. 2d shows, the summed experimental intensity distributions for the peak 1–3 were divided by a normalization factor for a best match with the corresponding theoretical one, and then this factor was commonly used to normalize the experimental momentum distributions of all outer valence orbitals. The $2b_1$ theoretical momentum profile calculated using the HF/Aug-cc-pVTZ method was also compared with the experimental momentum distributions of the outermost peak in Fig. 2a. It is obvious that the $2b_1$ assignment can not describe the observed distribution, while the

$7b_2$ can. Therefore, the outermost peak can be unanimously assigned to the valence $7b_2$ orbital. It should be noted that the electronic correlation has been partly considered through the exchange–correlation potentials in the B3LYP calculations. Therefore, the B3LYP theoretical curves described the experimental distributions better than the HF results. Fig. 2b shows the momentum distributions of the orbital $2b_1$ at 10.5 eV. The experimental momentum distributions are in good agreement with the theoretical calculations when the latter is scaled by a factor of 0.8, which representing the pole strength of $2b_1$. As a result, it is 20% less than the pole strength of the outermost orbital because the normalization procedure used in present work means that the pole strength of the outermost orbital is one, while ADC(3)/6–31G method predicted almost the same pole strengths for these four outermost orbitals [10]. It is unlikely caused by an experimental artifact because both the factors at 1500 eV and at 600 eV were less than one. The possible reason is that the ADC(3) calculation employed a quite limited basis set of 6–31G and the higher order electronic correlations were not taken into account; therefore, it cannot accurately reproduce the observed results [22]. The discrepancy between experimental results and theoretical ones at the low momentum region $p < 0.3$ a.u. may be ascribed to some dynamical effects because it diminished at a much higher impact energy of 1500 eV, as shown in Fig. 2b. Moreover, it is interesting to note that

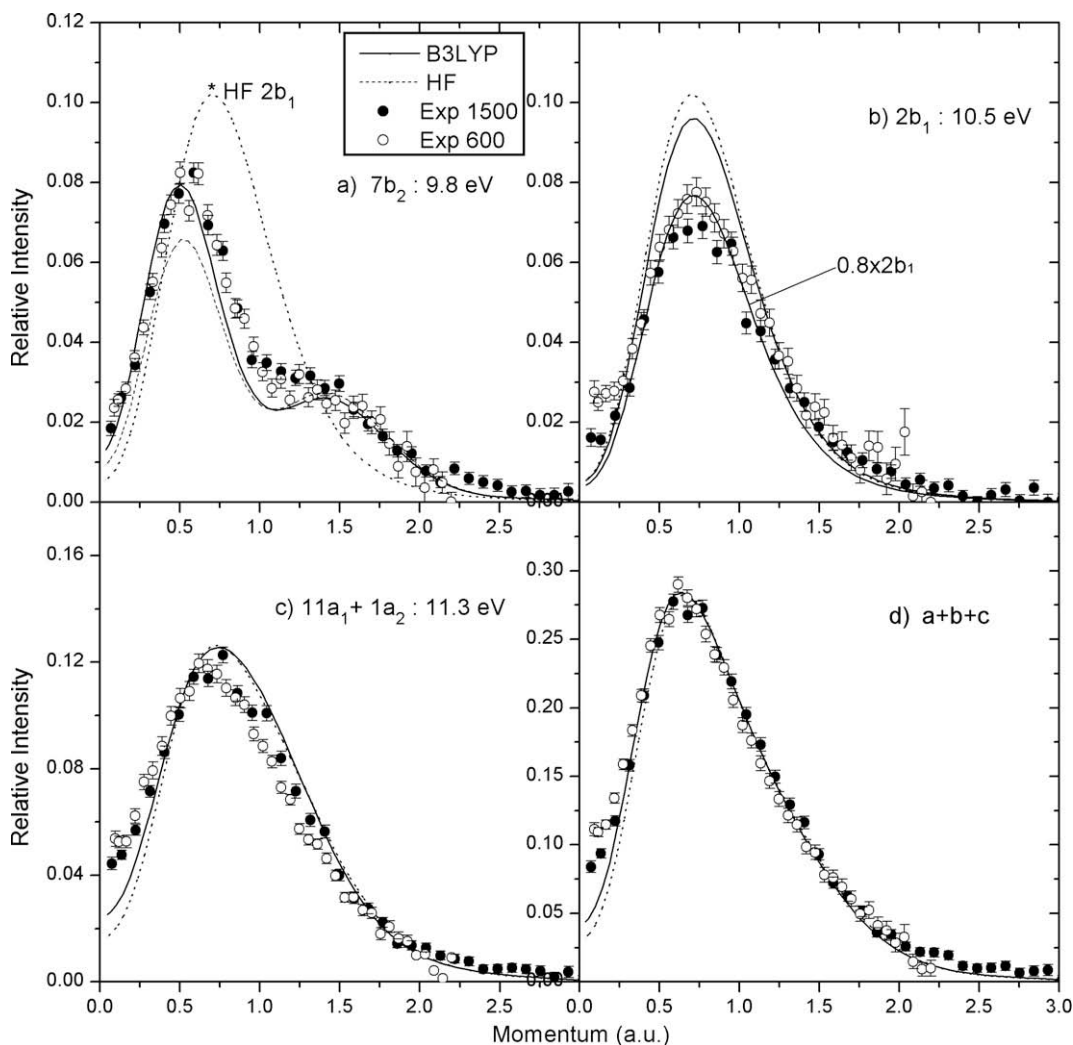


Fig. 2. Spherically averaged momentum distribution of the outer valence orbitals in the binding energy region between 8 eV and 12 eV of pyrimidine at impact energy of 1500 eV and 600 eV. The curve labeled with 'HF $2b_1$ ', the calculated result with the Hartree–Fock method, was compared in order to reflect the incorrect orbital order given by the Hartree–Fock method.

$2b_1$ is a d-like orbital, as shown in Fig. 3. This phenomenon is similar to our recent observations in oxygen [17], and ethylene molecules [18].

The severe overlap on the binding energy spectra makes difficult obtaining the experimental momentum distributions for the outer valence orbitals individually. Therefore, the other six outer valence orbitals in the binding energy region of 12–18 eV were grouped into three bands, which were located at 14.1 eV, 15.7 eV and 17.5 eV, respectively. The summed experimental intensity distributions related to the band $10a_1 + 1b_1 + 6b_2$ (14.1 eV) are compared with the theoretical distributions in Fig. 4a. It can be seen that both the theoretical methods can well describe the experimental profiles in general. It should be noted that there exists a non-neglectable discrepancy in the region around $p = 0.5$ a.u. between the experimental results at the impact energies of 1500 eV and that at 600 eV. The experimental intensity at 600 eV is higher than that at 1500 eV in the momentum region around $p = 0.5$ a.u. Fig. 4b shows the comparison between the experimental momentum distributions of the orbital $9a_1$ (15.7 eV) and the theoretical momentum distributions. Although the theories predicted a similar profile to the experimental distribution at 1500 eV and that at 600 eV. As for the band $8a_1 + 5b_2$ (17.5 eV), the experimental momentum distributions at both impact energies are almost the same, as shown in Fig. 4c, and the theoretical calculations can well reproduce the observed distributions except in the region around $p = 0.5$ a.u., where the experimental intensity were evidently underestimated. Since there are some overlaps among the three bands in Fig. 2, one might ascribe the discrepancies to

the intensity leakage from the neighbor orbitals. Therefore, their summed intensity distributions were compared in Fig. 4d to check this possibility. It can be seen that the discrepancies in lower momentum region $p < 0.5$ a.u. still exist, and the experimental distributions in lower momentum region depends on the impact energies. Considering the similarity to $2b_1$ orbital, one may tentatively ascribe it to the distorted wave effects. However, it should be noted that none of these outer valence orbitals ($10a_1$, $1b_1$, $6b_2$, $9a_1$, $8a_1$, $5b_2$) is d-like, as Fig. 3 shows. It is still a challenge to perform the calculation using the distorted wave impulse approximation (DWIA) due to the multi-center of a molecular target and the size as big as the pyrimidine molecule. Since the PWIA fails in most d-like orbital cases, it is naturally to ask what will happen for the orbital with a higher angular momentum quantum number, such as f-like, g-like. If we expand the multi-center electronic wavefunction using the single center functions, the components with higher angular momentum quantum numbers will have significant weights for the ring or cage molecules with a high symmetry. It is interesting to note that the $5b_2$ orbital is f-like (see Fig. 3). However, since the intensity of $8a_1$ is one order in magnitude higher than that of $5b_2$ in the low momentum region, their summed experimental intensity distributions cannot provide a definitive conclusion. The dependence on impact energies of experimental momentum distributions was observed also in our recent (e, 2e) experiment on the SF_6 sample at various impact energies for the orbitals with a higher angular momentum quantum number [27]. Such effects are worthy of further investigations considering the widely applications of the (e, 2e) spectroscopy. It should be very cautious in using the (e, 2e) reaction to investigate the molecular conformation population by comparing the PWIA theoretical results with the experimental results at a single impact energy. Re-

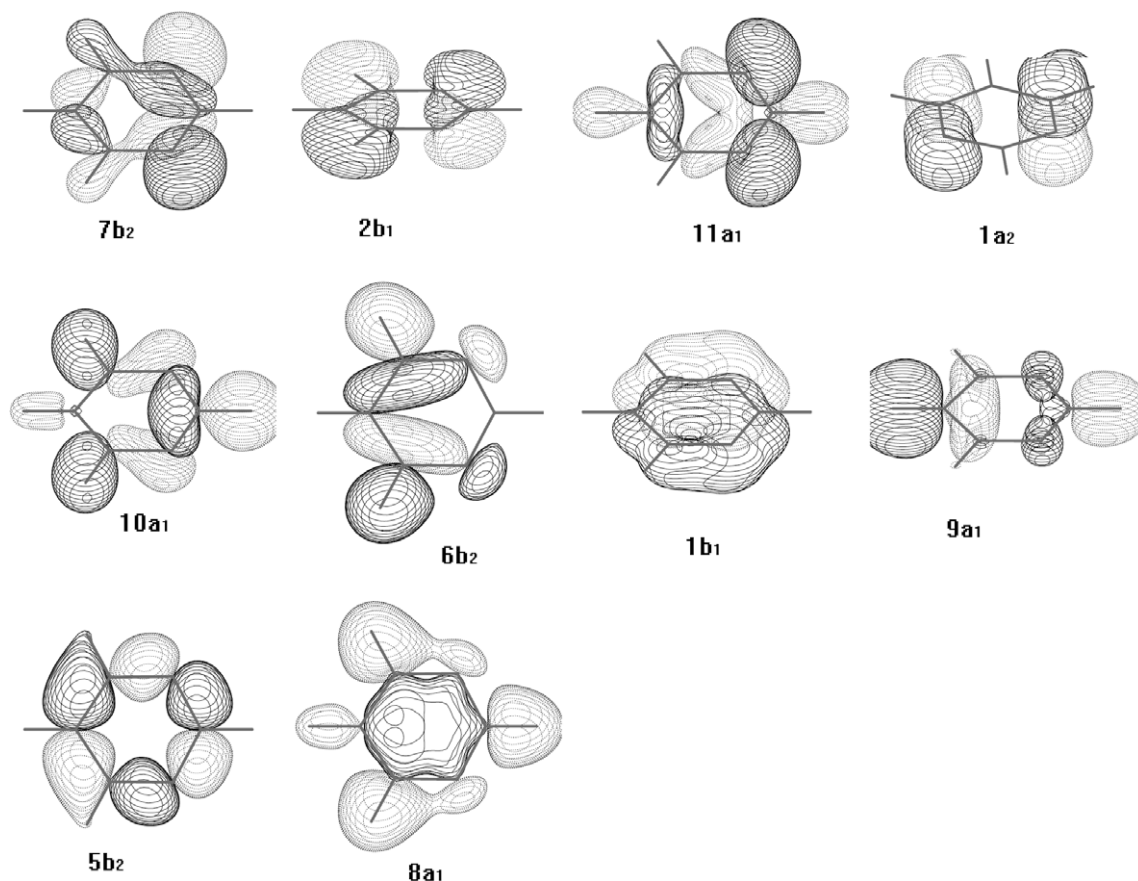


Fig. 3. The density contour plots of the outer valence orbitals of pyrimidine. The displayed molecular orbitals were drawn using MOLDEN 4.3 with a density contour value of 0.05 [30].

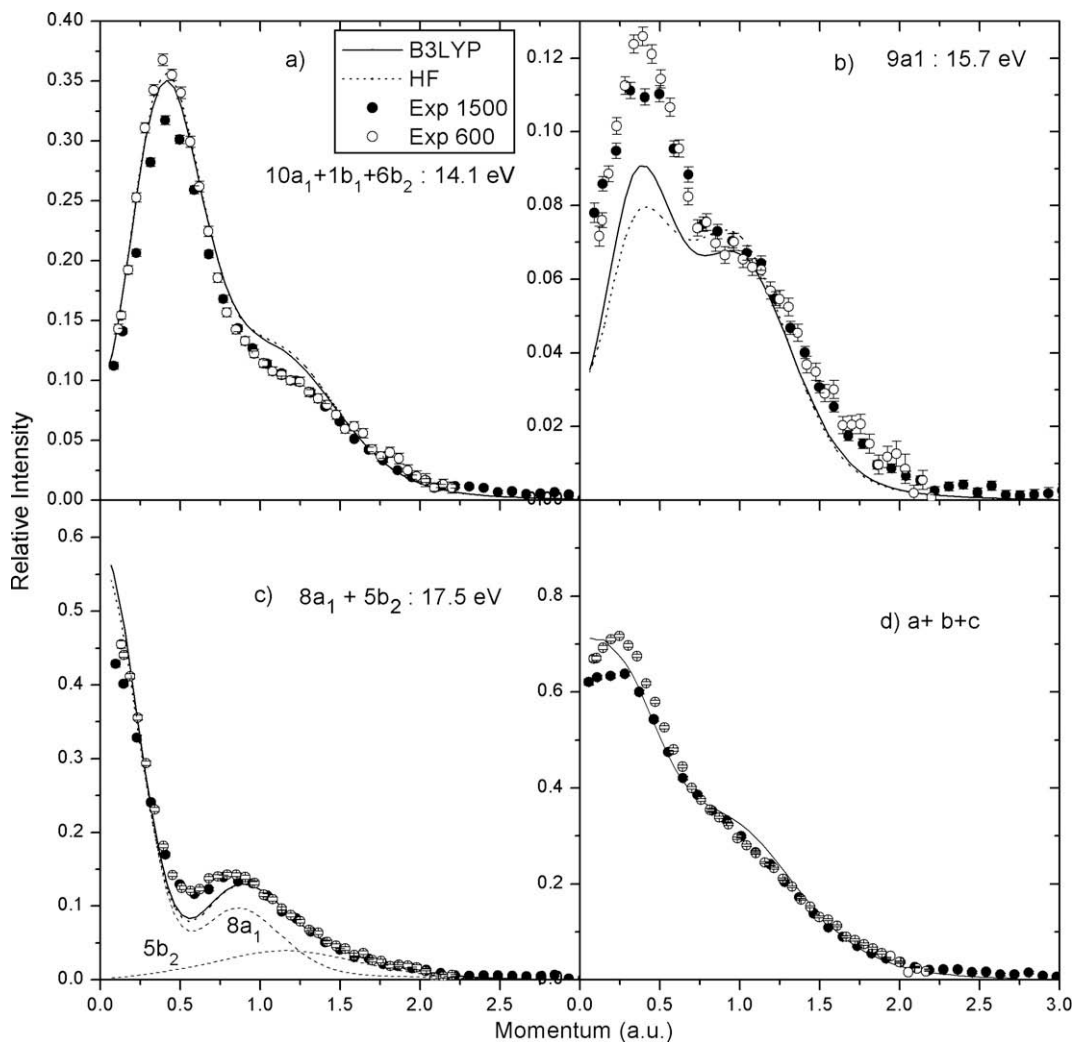


Fig. 4. Spherically averaged momentum distribution of the outer valence orbitals in the binding energy region between 12 eV and 19 eV of pyrimidine at impact energy of 1500 eV and 600 eV. The calculated momentum distributions of orbital $8a_1$ and $5b_2$ were illustrated with the dash curves in the panel (c) with the B3LYP method.

cently, Madison et al. have reported DWIA calculations for the ($e, 2e$) reaction on hydrogen [28] and nitrogen molecules [29]. The combination of the high level DWIA calculations with the benchmark experiments on some typical molecules with a high symmetry may answer this question in the near future.

The continuous background in the inner valence region (>20 eV) in Fig. 2 is the result of the breakdown of the single orbital picture. The assignments for the peaks were tentatively presented incorporating with the theoretical results, especially the DFT results corrected by statistical average of orbital potential (SAOP) method [31]. The peak located at 20.6 eV, which has a p-type momentum profile, is the main line of the band $7a_1 + 4b_2$, while $6a_1$ was assigned to the peak at 24.5 eV, $3b_2$ to 26.2 eV, $5a_1$ to 29.3 eV, respectively. The detailed interpretation needs high level many-body calculations.

4. Conclusions

The valence orbitals of pyrimidine were investigated using the high resolution electron momentum spectroscopy incorporating with the HF, B3LYP and OVGf theoretical calculations. The comparisons between experimental momentum distributions and theoretical ones provided an unambiguous orbital assignment. The highest occupied molecular orbital (HOMO) was assigned to $7b_2$

symmetry. It was found that the pole strength of the next highest occupied molecular orbital, $2b_1$, was around 0.8. Moreover, the evident difference between the momentum distributions at 1500 eV and that at 600 eV was observed, which showed the limitation of the PWIA for some orbitals of pyrimidine. The present study indicated that we should be very cautious in using the ($e, 2e$) reaction to investigate the molecular conformational population by comparing the PWIA theoretical results with the experimental results at a single impact energy. Such effects are worthy of the further investigations considering the widely applications of the ($e, 2e$) spectroscopy.

Acknowledgements

This work is supported by the National Natural Science Foundation of China under Contract Nos. 10704046, 10874097 and 10575062, and Specialized Research Fund for the Doctoral Program of Higher Education under 20070003146.

References

- [1] F. Wang, M.T. Downton, N. Kidwani, J. Theo. Comp. Chem. 4 (2005) 247.
- [2] C.T. Falzon, F. Wang, W.N. Pang, J. Phys. Chem. B 110 (2006) 9713.
- [3] D.M.P. Holland, A.W. Potts, L. Karlsson, I.L. Zaytseva, A.B. Trofimov, J. Schirmer, Chem. Phys. 353 (2008) 47 (and references therein).

- [4] E. Weigold, I.E. McCarthy, *Electron Momentum Spectroscopy*, Kluwer/Plenum, New York, 1999.
- [5] C.E. Brion, *Int. J. Quantum Chem.* 29 (1986) 1397.
- [6] Y. Zheng, J.J. Neville, C.E. Brion, *Science* 270 (1995) 786.
- [7] M.N. Piancastelli, P.R. Keller, J.W. Taylor, F.A. Grimm, T.A. Carlson, *J. Am. Chem. Soc.* 105 (1983) 4235.
- [8] L. Asbrink, C. Fridh, B.Ö. Jonsson, E. Lindholm, *Int. J. Mass Spectrom. Ion Phys.* 8 (1972) 215.
- [9] W. von Niessen, W.P. Kraemer, G.H.F. Diercksen, *Chem. Phys.* 41 (1979) 113.
- [10] A.W. Potts, D.M.P. Holland, A.B. Trofimov, J. Schirmer, L. Karlsson, K. Siegbahn, *J. Phys. B: At. Mol. Opt. Phys.* 36 (2003) 3129.
- [11] U. Lottermoser, P. Rademacher, M. Mazik, K. Kowski, *Eur. J. Org. Chem.* (2005) 522.
- [12] G. Cooper, W.Z. Zhang, C.E. Brion, *Chem. Phys.* 145 (1990) 117.
- [13] C.G. Ning, X.G. Ren, J.K. Deng, G.L. Su, S.F. Zhang, F. Huang, G.Q. Li, *Chin. Phys.* 14 (2005) 2467.
- [14] X. Shan, X.J. Chen, L.X. Zhou, Z.J. Li, T. Liu, X.X. Xue, K.Z. Xu, *J. Chem. Phys.* 125 (2006) 154307.
- [15] X.G. Ren, C.G. Ning, J.K. Deng, S.F. Zhang, G.L. Su, F. Huang, G.Q. Li, *Rev. Sci. Instrum.* 76 (2005) 063103.
- [16] C.G. Ning, S.F. Zhang, J.K. Deng, K. Liu, Y.R. Huang, Z.H. Luo, *Chin. Phys.* 17 (2008) 1674.
- [17] C.G. Ning, X.G. Ren, J.K. Deng, G.L. Su, S.F. Zhang, G.Q. Li, *Phys. Rev. A* 73 (2006) 022704.
- [18] X.G. Ren, C.G. Ning, J.K. Deng, S.F. Zhang, G.L. Su, F. Huang, G.Q. Li, *Phys. Rev. Lett.* 94 (2005) 163201.
- [19] P. Duffy, D.P. Chong, M.E. Casida, D.R. Salahub, *Phys. Rev. A* 50 (1994) 4704.
- [20] Y. Zheng et al., *Chem. Phys.* 212 (1996) 269.
- [21] M.J. Frisch et al., *GAUSSIAN 98*, Gaussian Inc., Pittsburgh, PA, 1998.
- [22] C.G. Ning et al., *Chem. Phys.* 343 (2008) 19.
- [23] C. Lee, W. Yang, R.G. Parr, *Phys. Rev. B* 37 (1988) 785.
- [24] W. von Niessen, J. Schirmer, L.S. Cederbaum, *Comput. Phys. Rep.* 1 (1984) 57.
- [25] J.V. Ortiz, *J. Chem. Phys.* 89 (1988) 6348.
- [26] P. Duffy, M.E. Casida, C.E. Brion, D.P. Chong, *Chem. Phys.* 159 (1992) 347.
- [27] A paper in preparation.
- [28] J.F. Gao, D.H. Madison, J.L. Peacher, A.J. Murray, M.J. Hussey, *J. Chem. Phys.* 124 (2006) 194306.
- [29] J.F. Gao, D.H. Madison, J.L. Peacher, *Phys. Rev. A* 72 (2005) 020701.
- [30] G. Schaftenaar, J.H. Noordik, *J. Comput.-Aided Mol. Des.* 14 (2000) 123.
- [31] D.P. Chong, O.V. Gritsenko, E.J. Baerends, *J. Chem. Phys.* 116 (2002) 1760.